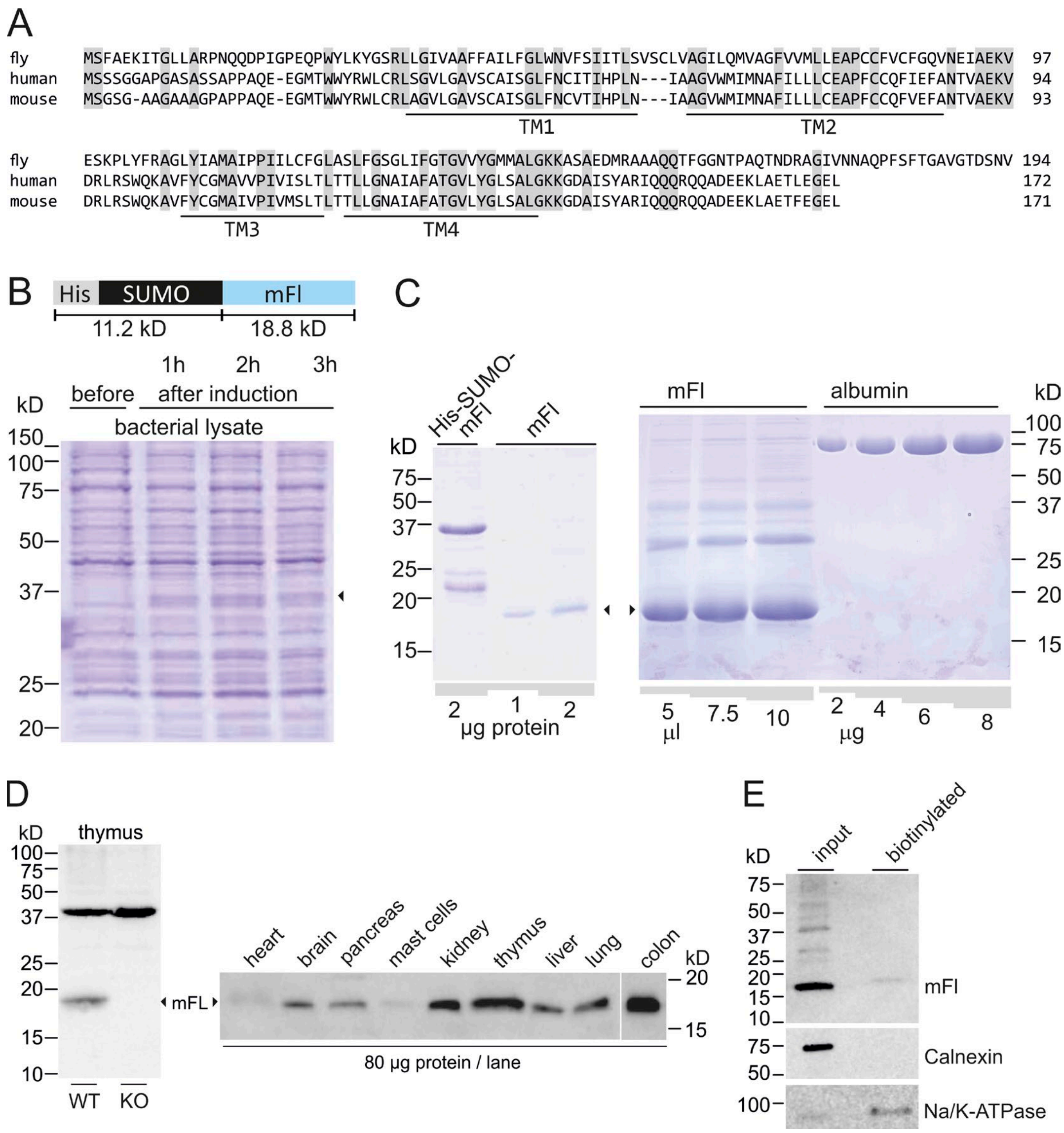

Figure S1. **Generation of antibody for the mouse Flower protein (mFl).** **(A)** Alignment of amino acid sequences of Flower from *Drosophila* (fly; NCBI accession no. NP_648804.1), human (NP_060056.1), and mouse (NM_029862). Identical amino acids are highlighted in gray. Transmembrane domains (TM1 to TM4) predicted from the hydropathy profile (window size 19; Kyte and Doolittle, 1982) of the mouse protein are indicated. **(B)** The mFl cDNA was subcloned 3′ and in frame to His$_6$-SUMO cDNA into the prokaryotic pCA528 expression vector (provided by G. Schlenstedt [Saarland University, Homburg, Germany]) and expressed as a fusion protein in *E. coli* Rosetta (DE3)-pLysS. Shown is a Coomassie-stained 12% SDS gel with bacterial lysate before and after induction with 1 mM IPTG; the His$_6$-SUMO-mFl is indicated by the arrowhead. **(C)** Coomassie stained 15% SDS gel with purified His$_6$-SUMO-mFl and purified mFl (left; 1 and 2 µg per lane) and quantification of recombinant mFl relative to BSA (right). Proteins from bacterial pellets were obtained as described (Trentmann et al., 2007) and solubilized in the presence of 0.1% dodecyl-β-D-maltosid. The solubilized His$_6$-SUMO-mFl was purified by IMAC (Ni Sepharose 6 Fast Flow; Äkta Purifier FPLC Systems; GE Healthcare). The mFlower (indicated by the arrowhead) was obtained by His-tagged SUMO-protease Ulp1 cleavage of His$_6$-SUMO-mFl according to (Butt et al., 2005). On average, 7 mg recombinant mFl was obtained from 30 mg His$_6$-Sumo-mFl from 15 liter cultured *E. coli*. The recombinant protein was used to generate polyclonal anti-mFl antibodies in two rabbits according to Meissner et al. (2011). **(D)** Western blot of microsomal membrane proteins from the indicated tissues including thymus from mFl$^{-/-}$ (KO) mice by using the generated affinity-purified polyclonal antibody. The mFl protein is indicated by arrowheads. **(E)** Surface biotinylation of activated CTLs from WT mice. Western blot of input and proteins biotinylated at the cell surface by using antibodies for Flower (top), calnexin (middle, negative control for surface biotinylation), and the α1 subunit of the Na/K-ATPase (bottom, positive control for surface biotinylation). The Western blot was first incubated in the presence of anti-Flower, followed by incubation in the presence of anti-Calnexin and of anti-α1 Na/K-ATPase, respectively, after stripping the blot in between. Representative experiment of five independent experiments. Normalized to the input, 1.59 ± 0.23% of the Flower protein are biotinylated (mean ± SEM; $n = 5$; $P < 0.0001$; one sample *t* test), demonstrating that in activated CTLs only a very minor fraction of the Flower protein is associated with the plasma membrane. In comparison 19.55 ± 9.13% (mean ± SEM; $n = 3$; $P < 0.013$; one sample *t* test) of the α1 subunit of the Na/K-ATPase protein are biotinylated when normalized to input.

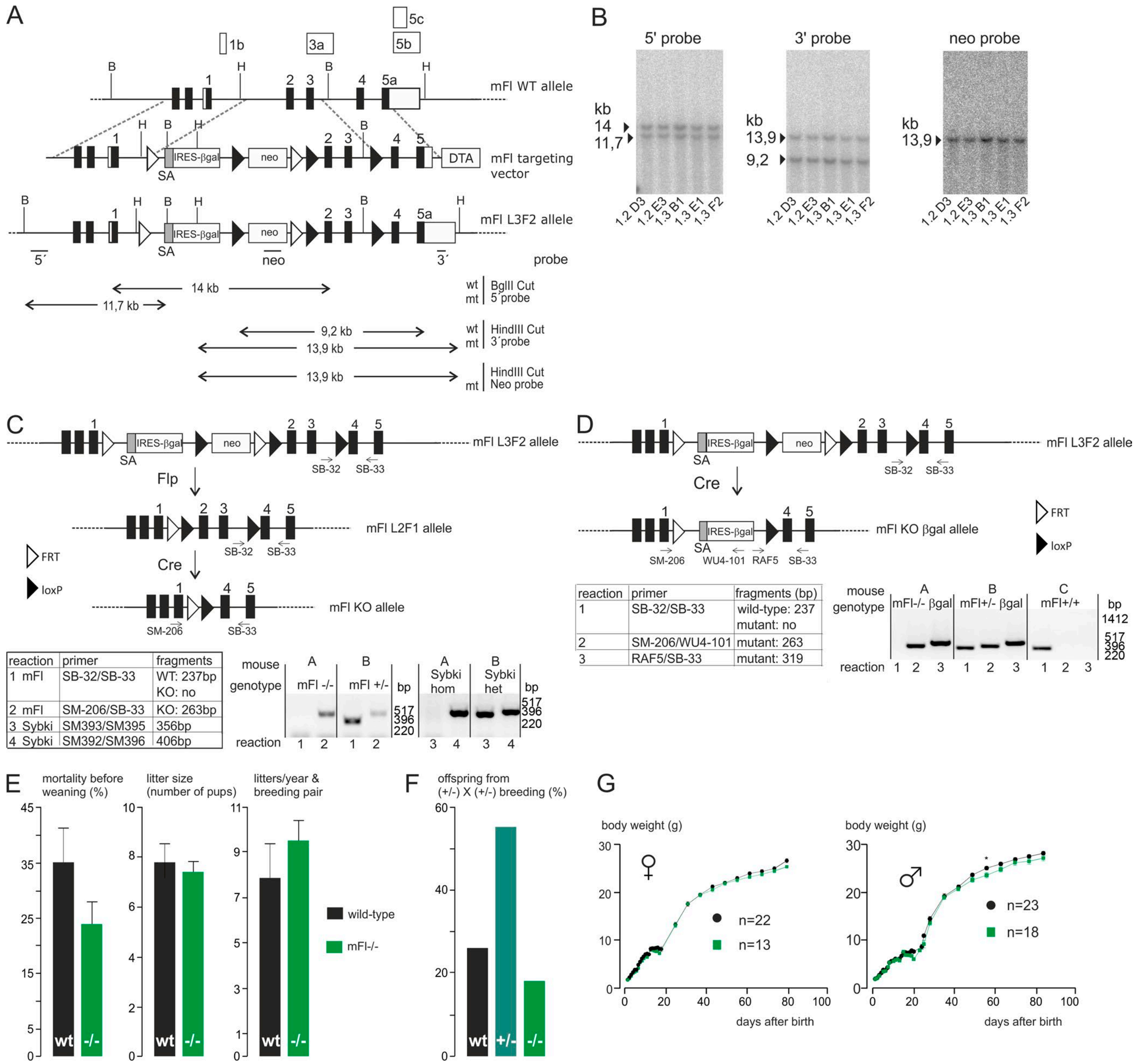

Figure S2. **Generation, verification, breeding performance, and body weight of Flower-deficient mice. (A)** Scheme of the nontranslated (open boxes) and translated exons (closed boxes; not in scale, taken from Ensembl Genome Browser). WT allele, targeting vector, and recombinant mFl L3F2 allele are shown. In the mFl L3F2 allele, exons 2 and 3 are flanked by loxP sites (closed triangles). 5′ of exon 2a SA-IRES-βGal cassette, a further loxP site, and a neo cassette all flanked by FRT sites (open triangles) are inserted. Probes and sizes of genomic DNA fragments as expected by Southern blots are indicated. B, BglII; H, HindIII. **(B)** Identification of the recombinant mFl L3F2 allele in ES cells by Southern blot by using a 5′probe (left) and 3′probe (middle) both placed external to the targeted sequence. The internal probe neo (right) indicates singular integration of the targeting vector. **(C)** Flp- and thereafter Cre-mediated conversion of the mFl L3F2 allele to the *mFl*$^{-/-}$ (*mFl KO*) allele and generation of Flower homozygous KO/Synaptobrevin2 mRFP-knock-in mice (*mFl*$^{-/-}$/*SybKI*$_{homozygous}$). The Synaptobrevin2 mRFP-knock-in mouse has been described (Matti et al., 2013). *SybKIhom*, *SybKI*$_{homozygous}$; *SybKIhet*, *SybKI*$_{heterozygous}$. The genotype was identified by genomic PCR, primers and fragment sizes as expected by PCR are depicted in the scheme and in the table, and primer sequences are shown in Table S4. **(D)** Cre-mediated recombination of the mFl L3F2 allele to the mFl KOβGal allele. **(E)** mFl$^{-/-}$ litters were analyzed regarding mortality between birth and weaning, litter size, and number of litters per breeding couple extrapolated to 1 yr (118 litters, 46 breedings). **(F)** Analysis of Mendelian inheritance of the mFl KO allele in heterozygous breedings (65 mice, eight litters of four breedings); not significant by Chi-square test. **(G)** C57BL/6N mice and mFl$^{-/-}$ mice were weighted over 80 d to monitor any body weight differences. Mean ± SEM with *n* (number of mice) and gender as indicated.

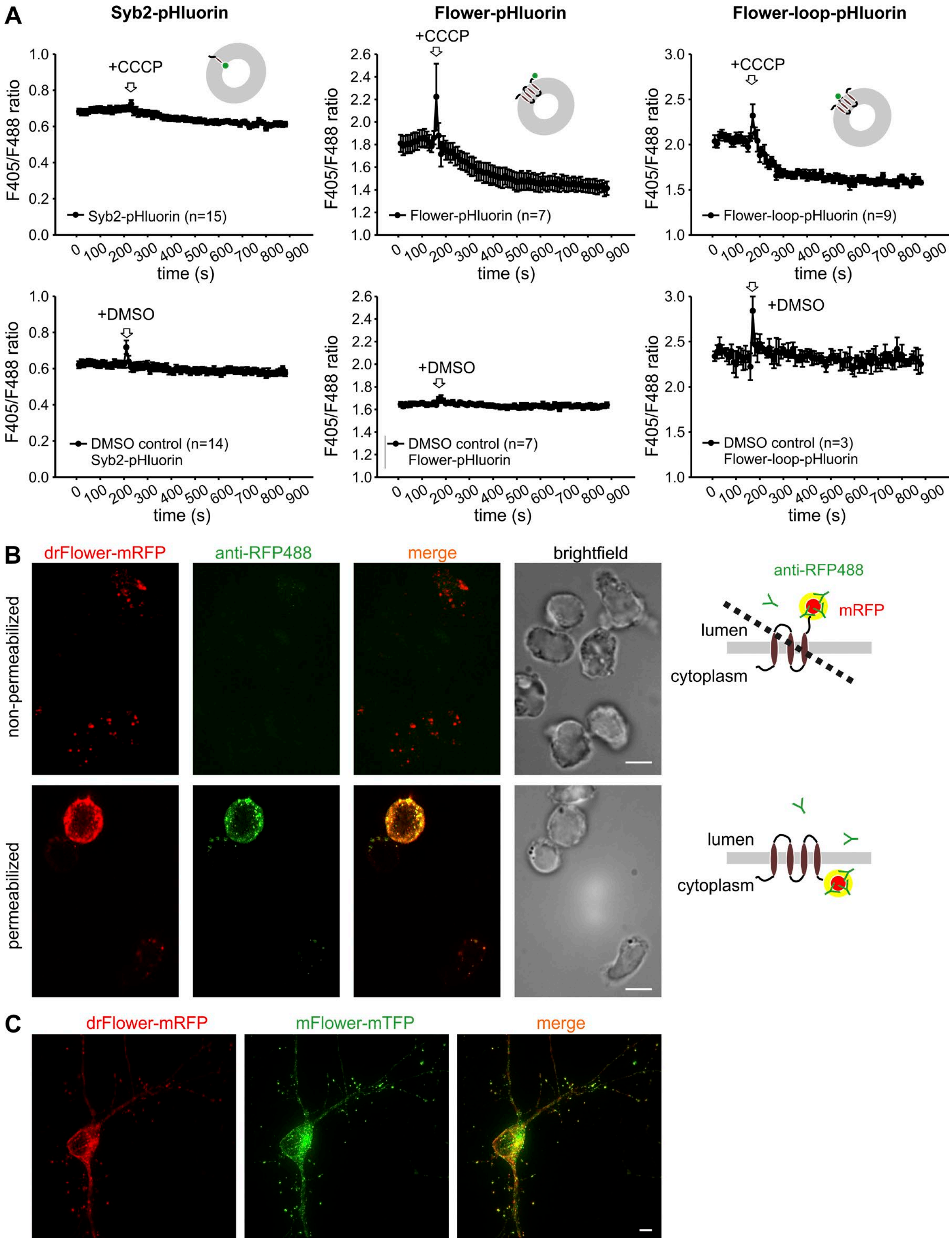

Figure S3. **Flower contains four transmembrane domains. (A)** CTLs were transfected with syb2-pHluorin (pHluorin fused to the luminal C terminus of Synaptobrevin2), Flower-pHluorin (pHluorin fused to the C terminus of Flower), and Flower-loop-pHluorin (pHluorin fused between the predicted second and third transmembrane segment of Flower). Cells were then imaged by confocal microscopy before and after applying 50 μM CCCP to acidify the cytosol. Excitation was at 405 and 488 nm and emission measured at 515 nm. DMSO application was used as the control (bottom). Data are given as mean ± SEM. **(B)** SIM images of CTLs transfected with *Drosophila* (dr) Flower-mRFP and stained with anti-RFP488 antibody before (top) and after permeabilization with 0.1% Triton X-100 (bottom). Bars, 5 μm. **(C)** SIM image of a hippocampal neuron transfected with constructs from *Drosophila* and mouse Flower fused to mRFP and mTFP, respectively. The merged image on the right shows a clear colocalization of both proteins. Bars, 5 μm.

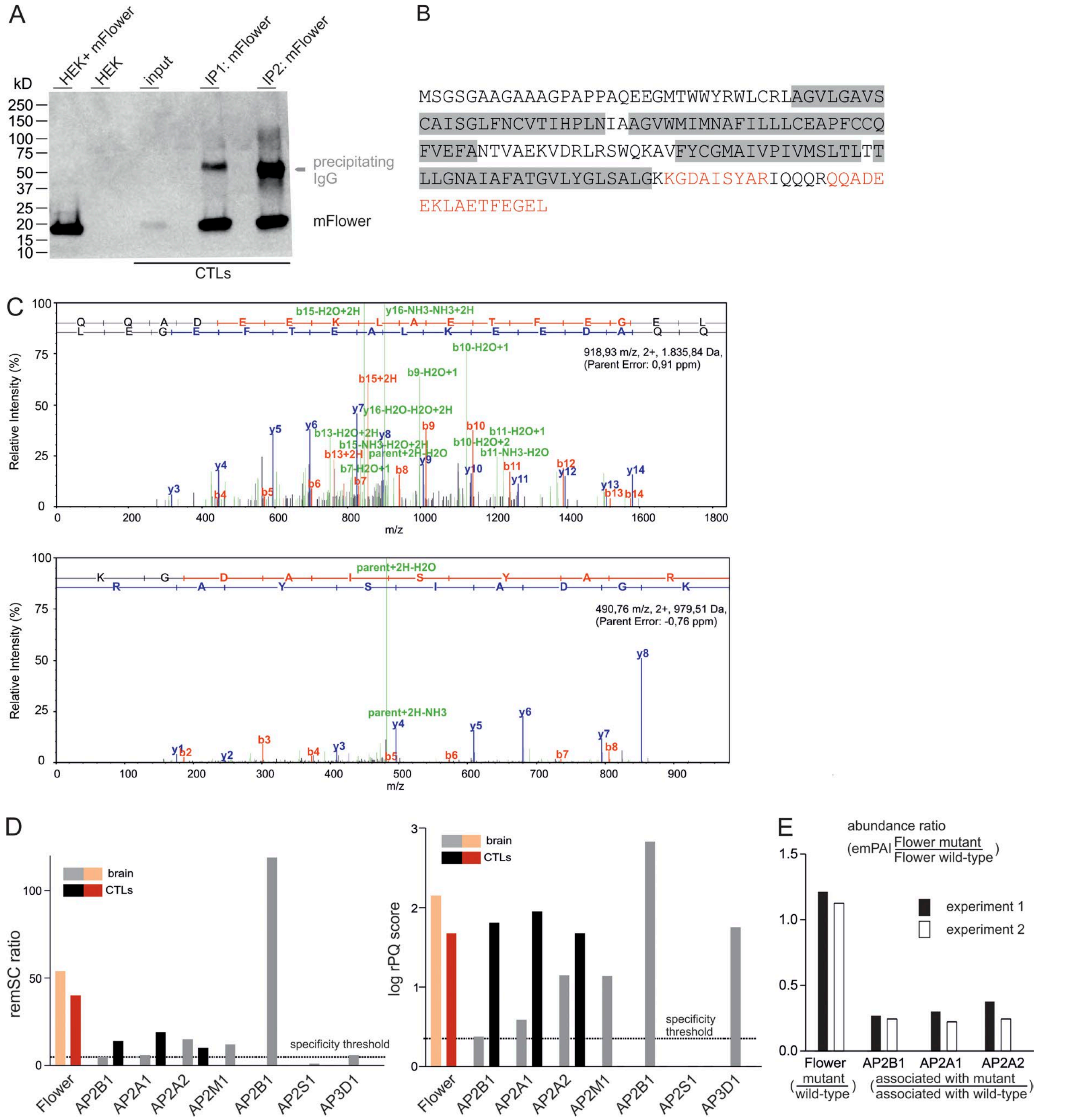

Figure S4. **Assembly of Flower with AP complexes. (A)** Western blot of protein aliquots eluted from the anti-Flower antibody after enrichment of the Flower-containing protein complexes from CTLs by using the anti-Flower antibody. Nontransfected HEK293 (HEK) and cells transfected with the mouse Flower cDNA (HEK+mFlower) served as the control. Input, aliquot of solubilized proteins before incubation with the anti-Fl antibody; IP1 and IP2, independent mFl antibody-based enrichments of Flower containing protein complexes. The ~18-kD Flower and the precipitating IgGs, recognized by the secondary anti–rabbit antibody, are indicated. **(B)** Proteins eluted from antibodies were separated on denaturing gels, in-gel trypsinized, and analyzed by nano-LC MS/MS. Primary sequence of the mouse Flower protein with the predicted transmembrane sequences shaded in gray. Amino acids of tryptic peptides identified with nano-LC MS/MS are in red (sequence coverage 15%). **(C)** MS/MS fragmentation spectra of tryptic peptides retrieved from the mouse Flower protein isolated from CTLs. **(D)** Histograms illustrating the distribution of the remSC ratio (left) and log rPQ score (right) of antibody-enriched proteins from brain and CTLs with corresponding specificity thresholds. Bars represent the enriched mFl protein from brain (yellow), CTLs (red) and the indicated AP proteins from brain (gray), and CTLs (black). The remSC ratio ($remSC_{IPmFl}/remSC_{IPIgG}$) and the log rPQ score calculated from the rPQ score (rPQ_{IPmFl}/rPQ_{IPIgG}) are shown. For proteins, which were not identified in the IgG control, the deviator value was set to 0.01. The dashed black line is the specificity threshold with log rPQ values >0.6. Similar results were obtained by quantification of peak volumes (mean of the three highest peptides areas measured for each protein, TOP^3 method; unpublished data). Data from nine independent analyses: CTLs with specific anti-Flower antibody (*n* = 2) and IgG control (*n* = 1); brain with specific mFlower antibody (*n* = 3) and IgG control (*n* = 3). **(E)** Abundance ratios of the TFP-tagged Flower or Flower-mutant protein were calculated from the normalized emPAI values (extracted from Scaffold) obtained in the enriched Flower-TFP or Flower mutant-TFP–containing protein complexes. Measurements were done twice (black bar, experiment 1; white bar, experiment 2). Flower-containing protein complexes were obtained from Flower gene-deficient CTLs, which were transfected with either WT Flower or Flower mutant cDNAs (both subcloned into the pMax vector); to ensure comparable antibody-based enrichment of both variants, TFP was fused to the C terminus, and the anti-TFP antibody (AB234; Evrogen Joint Stock Company) was used to enrich both proteins after lysis of the transfected cells and solubilization of membrane proteins. Thereafter the Flower containing protein complexes were analyzed by MS as described in Materials and methods.

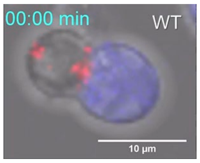

Video 1. **The specific block of endocytosis in CTLs from Flower-deficient mice by confocal microscopy.** Time-lapse maximal-intensity projections of syb2-mRFP (red) transfected CTLs conjugated to target cells in the presence of anti-RFP488 antibody (green) in the medium. 232 frames were collected and displayed at 24 frames/s. The corresponding still image is shown in Fig. 3 A.

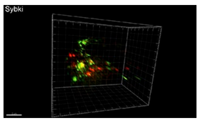

Video 2. **The 3D reconstruction of WT and Flower-deficient CTLs to demonstrate the block of endocytosis due to Flower deficiency.** 200-nm stack, 600 frames, 30 frames/s.

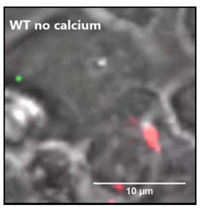

Video 3. **The rescue of the Flower phenotype by elevated calcium (confocal microscopy).** Time-lapse maximal-intensity projections of syb2-mRFP (red) transfected CTLs in contact with target cells before and after application of extracellular buffer containing 10 mM calcium. CTLs were incubated with target cells in the presence of anti-RFP488 antibody (green) in the medium for 30 min and then perfused with 10 mM calcium buffer. 117 frames were collected and displayed at 29 frames/s. The corresponding still image is shown in Fig. 5 A.

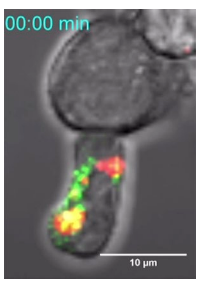

Video 4. **The polarization of Flower-containing vesicles to the IS before CG polarization (confocal microscopy).** Time-lapse maximal-intensity projections of a Flower-deficient CTL transfected with Flower-pHluorin (green) and syb2-mRFP (red) and conjugated to a target cell in the presence of anti-RFP405 antibody in the medium. 286 frames were collected and displayed at 25 frames/s. The corresponding still image is shown in the bottom row of Fig. 7 A.

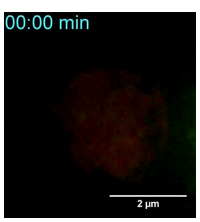

Video 5. **The polarization of Flower-containing vesicles to the IS before CG polarization (TIRFM).** Real-time dynamics of Flower-containing vesicles and CGs in CTL monitored by TIRFM. Flower-deficient CTLs were transfected with Flower-pHluorin (green) and syb2-mRFP (red). 1,000 frames were collected and displayed at 30 frames/s. The corresponding still image is shown in Fig. 7 B.

Table S1. **Flower and AP proteins affinity purified with anti-Flower antibody from brain and CTLs and identified by nano-LC MS/MS**

Protein ID (UniProtKB)	remSC(brain)	remSC(CTLs)	rPQ score (brain)	rPQ score (CTLs)
FLOWER (Q8BG21)	∞	∞	144	48
AP2B1 (Q9DBG3)	5	∞	2.49	64
AP2A1 (P17426)	6	∞	3.9	88
AP2A2 (P17427)	15	∞	14.3	48
AP2M1 (P84091)	12	—	14	—
AP1B1 (O35643)	∞	—	672	—
AP2S1 (P62743)	1	—	1	—
AP3D1 (O54774)	∞	—	56	—

For methods used for protein enrichment and MS, see Materials and methods. Values for remSC >5 and rPQ scores >4 refer to specific enrichment of AP proteins by anti-Flower antibody over negative control anti-IgGs. Number of experiments analyzed, n = 9: IPs from CTLs with specific mFlower antibody (n = 2) and IgG control (n = 1); IPs from brain with specific mFlower antibody (n = 3) and IgG control (n = 3).

Table S2. **Plasmids generated in the laboratories of the authors and used in this study**

Plasmid	mFl construct	Vector backbone	Comment
pSB_234	mFl_A	pcDNA3 (with STOP)	
pSB_235		pcDNA3 (without STOP)	
pSMa_79		pcAGGSM2-IRES-mRFP	
pSMa_80		pcAGGSM2-IRES dsRed-Express	
pSMa_91		pcAGGSM2-IRES-GFP	
pSMa_48	mFl_A-(R)pHluorin	pSFV1 (Semliki Forest Virus)	C-terminal fusion
pSB_123		pcAGGSM2	
pSMa_57	mFl_A-(S)pHluorin	pSFV1 (Semliki Forest Virus)	C-terminal fusion
pSMa_56		pcAGGSM2	
pSMa_59	mFl_B-(R)pHluorin	pcAGGSM2	C-terminal fusion
pSMa_61	mFl_D-(R)pHluorin	pcAGGSM2	C-terminal fusion
pSMa_62	mFl_E-(R)pHluorin	pcAGGSM2	C-terminal fusion
pSMa_63	mFl_A-mRFP	pcAGGSM2	C-terminal fusion
pSMa_64	mFl_B-mRFP	pcAGGSM2	C-terminal fusion
pSMa_66	mFl_D-mRFP	pcAGGSM2	C-terminal fusion
pSMa_67	mFl_E-mRFP	pcAGGSM2	C-terminal fusion
pSMa_68	mFl_B	pcAGGS-IRES-GFP	
pSMa_69	mFl_D	pcAGGS-IRES-GFP	
pSMa_70	mFl_E	pcAGGS-IRES-GFP	
pSMa_83	mFl_A-V50C	pcAGGS-IRES-GFP	V50C mutant mFl
pSMa_84	mFl_A-V50C-(R)pHluorin	pcAGGSM2	
pSMa_88	mFl_A-TM2-GFP-TM3	pcAGGSM2	GFP in the linker between TM2 and TM3
pSMa_89	(R)pHluorin-mFl_A	pcAGGSM2	N-terminal fusion
pSB_80	mFl_A-TM2-HA-TM3	pcAGGS-IRES-GFP	HA-Tag in the linker between TM2 and TM3
pSB_152	$mFl_{A\text{-}E74A}$	pcAGGS-IRES-GFP	E74A mutant
pSB_217	GCaMP6f-Gly_{10}-mFl_A(mut)	pcDNA3	N-terminal fusion
pSB_226		pcAGGS-IRES-TagRFP-T	
pSB_218	GCaMP6f-Gly_{10}-mFl_A(wt)	pcDNA3	N-terminal fusion
pSB_227		pcAGGS-IRES-TagRFP-T	
pSB_219	His-GCaMP6f-Gly_{10}-mFl_A(mut)	pcDNA3	N-terminal fusion
pSB_228		pcAGGS-IRES-TagRFP-T	
pSB_231		pMax-TagRFP-T	
pSB_282		pMax	
pSB_220	His-GCaMP6f-Gly_{10}-mFl_A(wt)	pcDNA3	N-terminal fusion
pSB_229		pcAGGS-IRES-TagRFP-T	
pSB_232		pMax-TagRFP-T	
pSB_283		pMax	
pSB_236	mFl_A-GST-Fusion	pcDNA3	
pSB_247	Fl_A	pMax-TagRFP-T	
pSB_248	Koz-mFl_A(wt)-(R)pHluorin- mFl_A(wt)-tagRFP-T	pMax-TagRFP-T	Tandem mFl_A cDNA with (R)pHluorin in between
pSB_249	mFl_A(wt)-GCaMP6f-mFl_A-tagRFP-T	pMax-TagRFP-T	Tandem mFl_A cDNA with GCaMP6f in between
pSB_272	Flower(TM1)-GCaMP6f	pMax	C-terminal fusion of mFl TM1 with GCaMP6f
pSB_273	Flower(TM1)-GCaMP6f-tagRFP-T-Stop	pMax	C-terminal fusion of mFl TM1 with GCaMP6f-tagRFP-T
pSB_274	Flower(TM1)-tagRFP-T	pMax	C-terminal fusion
pSB_343	mFl_A(wt)-mTFP	pMax	
pSB_344	mFl_A(mut)-mTFP	pMax	
	$drFl_A$-mRFP	pMax	
pSMa_92	TagRFP-T-mFl_A	pcAGGSM2	N-terminal fusion
pSB_353	mFl_A(mut)	pcAGGS-IRES-GFP	

The HisGCaMP6f and (R)pHlourine cDNAs have been described previously (Miesenböck et al., 1998; Chen et al., 2013). The *Drosophila* Flower cDNA ($drFl_A$; NCBI Reference Sequence: NM_140547.5) was codon optimized for *Mus musculus*, synthesized by Integrated DNA Technologies (Leuven), fused to mRFP, and subcloned into pMax. Fl_A, full-length mouse Flower cDNA encoding 171 amino acid residues (accession number NM_029862); mut, mutations introduced in Fl_A as indicated in Fig. 8 A; wt, WT Fl_A.

Table S3. **Antibodies used in this study**

Antibody	Supplier/reference	Identifier	Source
Anti-mouse flower	Generated in-house, this study	mFl	Rabbit pc
Anti-CD3e	BD Pharmingen	145-2C11	Hamster pc
Anti-CD107a-PE	BioLegend	1D4B	Rat pc
Anti-RFP	Genway Biotech	GWB-3BF-397	Rabbit, pc
Anti-TagRFP-t	Evrogen	AB234	Rabbit, pc
Anti-HA	Roche	3F10	Rat, mc
Anti-alpha1 Na^+/K^+-ATPase	Abcam	Ab 7671	Mouse mc
Anti-calnexin	Stressgen	SPA-865	Rabbit pc
Anti-GAPDH	Abcam	(6C5) ab 8245	Mouse mc
Anti-granzyme Alexa Fluor 647	BioLegend	AAN01	Mouse mc
Alexa Fluor–conjugated secondary anti-rabbit/mouse	Invitrogen	Alexa Fluor 488 Alexa Fluor 561 Alexa Fluor 647	Goat, pc
Secondary anti-rabbit	GE Healthcare	NA9340	Donkey
Secondary anti-mouse	GE Healthcare	NA9310	Sheep

The in-house generated antibody for mouse Flower is described in Materials and methods. mc, monoclonal; pc, polyclonal.

Table S4. **Oligodeoxynucleotide primers used for genotyping**

Identifier	Primers
WU4-101	5′-CGTTAATCTGATGCATGAGCC-3′
RAF5	5′-CACACCTCCCCCTGAACCTGAAAC-3′
SB-32	5′-GGATGAGTCAGTGTCTGTGC-3′
SB-33	5′-GGATGAGTCAGTGTCTGTGC-3′
SM-206	5′-GGATTTACAGCGACAGATGC-3′
SM-392	5′-GAGGGAAGGGATGTCAGCC-3′
SM-393	5′-GAAAGCTACCGTCACATACC-3′
SM-395	5′-AAGATATGGCTGAGAGGTGG-3′
SM-396	5′-TCACGTAGGCCTTGGAGCC-3′

References

Butt, T.R., S.C. Edavettal, J.P. Hall, and M.R. Mattern. 2005. SUMO fusion technology for difficult-to-express proteins. *Protein Expr. Purif.* 43:1–9. https://doi.org/10.1016/j.pep.2005.03.016

Chen, T.W., T.J. Wardill, Y. Sun, S.R. Pulver, S.L. Renninger, A. Baohan, E.R. Schreiter, R.A. Kerr, M.B. Orger, V. Jayaraman, et al. 2013. Ultrasensitive fluorescent proteins for imaging neuronal activity. *Nature.* 499:295–300. https://doi.org/10.1038/nature12354

Kyte, J., and R.F. Doolittle. 1982. A simple method for displaying the hydropathic character of a protein. *J. Mol. Biol.* 157:105–132. https://doi.org/10.1016/0022-2836(82)90515-0

Matti, U., V. Pattu, M. Halimani, C. Schirra, E. Krause, Y. Liu, L. Weins, H.F. Chang, R. Guzman, J. Olausson, et al. 2013. Synaptobrevin2 is the v-SNARE required for cytotoxic T-lymphocyte lytic granule fusion. *Nat. Commun.* 4:1439. https://doi.org/10.1038/ncomms2467

Meissner, M., V.C. Obmann, M. Hoschke, S. Link, M. Jung, G. Held, S.E. Philipp, R. Zimmermann, and V. Flockerzi. 2011. Lessons of studying TRP channels with antibodies. *In* TRP Channels. M.X. Zhu, editor. CRC Press, Boca Raton, FL. Chapter 6.

Miesenböck, G., D.A. De Angelis, and J.E. Rothman. 1998. Visualizing secretion and synaptic transmission with pH-sensitive green fluorescent proteins. *Nature.* 394:192–195. https://doi.org/10.1038/28190

Trentmann, O., M. Horn, A.C. van Scheltinga, H.E. Neuhaus, and I. Haferkamp. 2007. Enlightening energy parasitism by analysis of an ATP/ADP transporter from chlamydiae. *PLoS Biol.* 5:e231. https://doi.org/10.1371/journal.pbio.0050231